The Journal of Arthroplasty 29 (2014) 1491–1498

Contents lists available at ScienceDirect

The Journal of Arthroplasty

journal homepage: www.arthroplastyjournal.org

Load Sharing and Ligament Strains in Balanced, Overstuffed and Understuffed UKA. A Validated Finite Element Analysis

Bernardo Innocenti, PhD [a,b], Ömer Faruk Bilgen, MD [c], Luc Labey, PhD [a], G. Harry van Lenthe, PhD [d], Jos Vander Sloten, PhD [d], Fabio Catani, MD [e]

[a] European Centre for Knee Research, Smith&Nephew, Leuven, Belgium
[b] BEAMS Department, Université Libre de Bruxelles, Brussels, Belgium
[c] Department of Orthopaedia, School of Medicine, University of Uludağ, Bursa, Turkey
[d] Biomechanics Section, KU Leuven, Leuven, Belgium
[e] Orthopaedics and Traumatology Department, Modena Policlinic, Modena, Italy

ARTICLE INFO

Article history:
Received 4 October 2013
Accepted 20 January 2014

Keywords:
UKA
overstuffing
understuffing
tibial stress
collateral ligament strain

ABSTRACT

The aim of this study was to quantify the effects of understuffing and overstuffing UKA on bone stresses, load distribution and ligament strains. For that purpose, a numerical knee model of a cadaveric knee was developed and was validated against experimental measurements on that same knee. Good agreement was found among the numerical and experimental results. This study showed that, even if a medial UKA is well-aligned with normal soft tissue tension and with correct thickness of the tibia component, it induces a stiffness modification in the joint that alters the load distribution between the medial and lateral compartments, the bone stress and the ligament strain potentially leading to an osteoarthritic progression.

Osteoarthritis (OA) is the most common joint degeneration disease and affects a large part of the elderly population [1,2]. If OA is limited to only one compartment of the knee joint, usually the medial, a Unicompartmental Knee Arthroplasty (UKA) can relieve joint pain and restore function for properly selected patients [3,4].

Although several clinical studies suggest that the knee after UKA can reproduce the motion of the intact knee [3–6], and several authors have reported excellent results at 10 years of follow-up with modern designs [5–8], some cases of failure are also described in the literature [9,10]. In general, besides wear [11,12], four main postoperative problems are reported in the literature [13,14]: i. loosening of the prosthesis component (femoral and most frequently tibial), due to stress shielding in the bone [7,14,15]; ii. malpositioning of prosthetic components, which could lead to failure in the fixation of the implant to the bone due to an excessive bone stress and an increase in the strains in the soft tissues [4,16–18]; iii. medial knee pain, which is related to bone overload, components malpositioning and soft tissue tensioning [16,19]; iv. OA progression in the lateral side due to an altered stress pattern in the bone/cartilage [7,20].

Therefore, the knowledge of the stresses in the bone and strains in soft structures and the joint after the implantation of a UKA is important to study the implant behavior in the patient. UKA is a technically demanding surgical procedure, and care must be taken with component sizing, bone cuts and postoperative alignment as overstuffing or understuffing the joint could lead to inferior results [21–24]. Understuffing and overstuffing can be often seen during surgery leading to a slackening or a tightening of the medial soft tissue structure [21–24]. Furthermore such configurations induce an altered stress distribution in the tibial bone and have an effect on the load distribution between the medial and lateral side of the knee joint [9,25].

For these reasons, the aims of this study were:

- to develop, analyze and validate a patient specific finite element model of an intact knee joint before and after a UKA surgery;
- to investigate the change of stress distribution in the proximal tibia, strains in the collateral ligaments and the load distribution between the medial and lateral compartment will be investigated before and after a insertion of UKA. Three different conditions will be investigated: the optimal balanced and aligned UKA configuration, achieved using an optimal polyethylene insert thickness, and several overstuffed and understuffed UKA configurations achieved using thicker or thinner tibial polyethylene thickness.

The Conflict of Interest statement associated with this article can be found at http://dx.doi.org/10.1016/j.arth.2014.01.020.

Reprint requests: Bernardo Innocenti, Ph.D., Université Libre de Bruxelles, École polytechnique de Bruxelles, BEAMS Department (Bio Electro and Mechanical Systems), Av. F. Roosevelt, 50 CP165/56, 1050 Bruxelles, Belgium.

http://dx.doi.org/10.1016/j.arth.2014.01.020
0883-5403/

Material and Methods

Healthy Knee Model

The healthy knee model geometry was determined on Computed Tomography (CT) and Magnetic Resonance Imaging (MRI) scans of one intact fresh-frozen left native knee cadaveric specimen. The specimen did not display any deformity of the joint. In particular, to identify the bone, a helical CT scan was used (CT setting: 120 kV, 450 mA, slice thickness of 1.25 mm and a pitch of 0.5 mm/rev) while, to identify cartilage, menisci and soft tissue insertion points an MRI was performed (MRI setting: TE: 32 ms, TR: 4450 ms, slice thickness: 2 mm, flip angle 90°, NEX: 2 and FOV: 22 cm). The CT and MR images were imported in an image processing software (Mimics 13.1, Materialise, Leuven, BE) to extract the geometry and to generate 3D models of all the structures [16,26,27]. Two numerical models of the healthy knee were defined. The first comprised the following structures: menisci, cancellous bone, cortical bone and cartilage of tibial and femur. The second one included also the collateral ligaments. The cruciate ligaments were omitted in the FE models because the knee was placed in full extension and internal/external rotation was constrained during the tests.

Linear elasticity was used for all the material models considered in this study; values were taken from the literature [28,29].

According to literature [30], the cortical and cancellous bone was considered transversely isotropic (Table 1). The articular cartilage and the menisci were considered linear isotropic with respectively E=12 MPa, ν=0.45 [31–34] and E=8 MPa, ν=0.45 [35,36]. Because one of the aims of this study was to analyze the change in strain in the soft tissues after insertion and malpositioning of the UKA, the anterior and posterior medial collateral ligaments (aMCL and pMCL) as well as the lateral collateral ligament (LCL) were incorporated in the FE models of this study. The behavior of the ligaments was assumed linear elastic isotropic [26,27,37,38]. Each ligament was modeled as a beam with a specific cross-sectional area [26,27,39]. An initial preload was set for each ligament [32–35,40]. The origin and the insertion points of each collateral ligament were determined from the MR images [41,42]. The full overview of the properties of each ligament is given in Table 2.

A coefficient of friction of 0.001 was considered for the contact cartilage–cartilage, while a coefficient of friction of 0.01 was selected for the interface between the cartilage and the menisci [34,43].

UKA Knee Model

Once the healthy knee model was developed, a fixed bearing metal-backed UKA (Accuris, Smith&Nephew, Memphis, TN) was selected and virtually implanted, following the manufacturer's surgical technique, in the medial compartment of the knee models (both with and without collateral ligaments). According to the dimension of the femur and the tibia a size large was chosen for both the femoral component and tibial tray. Five different configurations were adopted in this study:

- balanced configuration according to the manufacturer's guidelines, that represents a balanced knee joint, was achieved using a tibial articular insert with a thickness of 10 mm. Such thickness included the polyethylene (8 mm) and the tibial tray thickness (2 mm). This implantation was confirmed by an experienced surgeon.
- Overstuffed configurations were simulated by implanting tibial articular inserts with a thickness of 11 mm and 12 mm;
- Understuffed configurations were simulated by implanting tibial articular inserts with a thickness of 9 mm and 8 mm (Fig. 1).

In Fig. 1 the healthy configuration, together with the UKA balanced configuration and the overstuffing (12 mm) and understuffing (8 mm) configurations are shown.

The material of the femoral component, tibial tray and tibial insert was respectively oxidized zirconium (Oxinium), titanium alloy (Ti6Al4V) an ultra-high-molecular-weight-polyethylene (UHMWPE). Similar to the previous selection, also in this case, the materials were assumed to be homogeneous, isotropic, and linear elastic [19,44,45]. The material properties were: Oxinium: E=97.900 MPa, ν=0.3 [42,45–47]; Titanium: E=117.000 MPa, ν=0.3[39,45]; UHMWPE: E=685 MPa, ν=0.4 [28,46–48];

A coefficient of friction of 0.04 was considered for the interaction between the femoral component and the tibial insert [19,29,46,49]. The interfaces between prosthetic components and bone were rigidly fixed simulating the use of cement [16].

Load and Boundary Conditions

Each knee configuration underwent a vertical compression force, applied with the knee in full extension, of 2000 N, similar to several previous studies [28,49,50]. This value corresponds to 2.55 times the body weight of a person having a mass of 80 kg and it is equivalent to the maximal axial force during gait [16,51]. In all the tests, the tibial bone was completely fixed at its distal end [35,45,48].

Finite Element Analysis

Each model was meshed using tetrahedral elements with an approximate element size of 1 mm. A convergence test was performed to check the element size mesh quality. Abaqus/Standard version 6.10-1 (Dassault Systèmes, Vélizy-Villacoublay, France) was used to perform all the finite element simulations.

For all the defined models (the intact knee and the five replaced models), the Von Mises stress in the proximal tibia, the strains in the collateral ligaments and the load distribution between the medial and lateral compartment were extracted.

Experimental Model for Validation

To allow the validation of the outcomes of numerical models, experimental tests were performed with the fresh-frozen cadaver knee on which the numerical model was based. Identical load and boundary conditions of the numerical model were applied.

Table 2
Material Properties of the Ligaments.

Ligaments	Young's Modulus [MPa]	Poisson's Ratio	Initial Strain εr	Cross-Sectional Area [mm^2]
LCL	111	0.45	0.05	18
aMCL	196	0.45	0.04	14
pMCL	196	0.45	0.03	14

Table 1
Material Properties for Cortical and Cancellous Bone; the First Axis Was Taken Parallel With the Anatomical Axis of the Bone.

		Young's Modulus [MPa]			Poisson's Ratio		
Material	Material Model	E_1	E_2	E_3	ν_{12}	ν_{13}	ν_{23}
Cortical bone	Transversely Isotropic	17,800	9600	9600	.30	.30	.55
Cancellous bone	Transversely Isotropic	344	99	99	.38	.38	.23

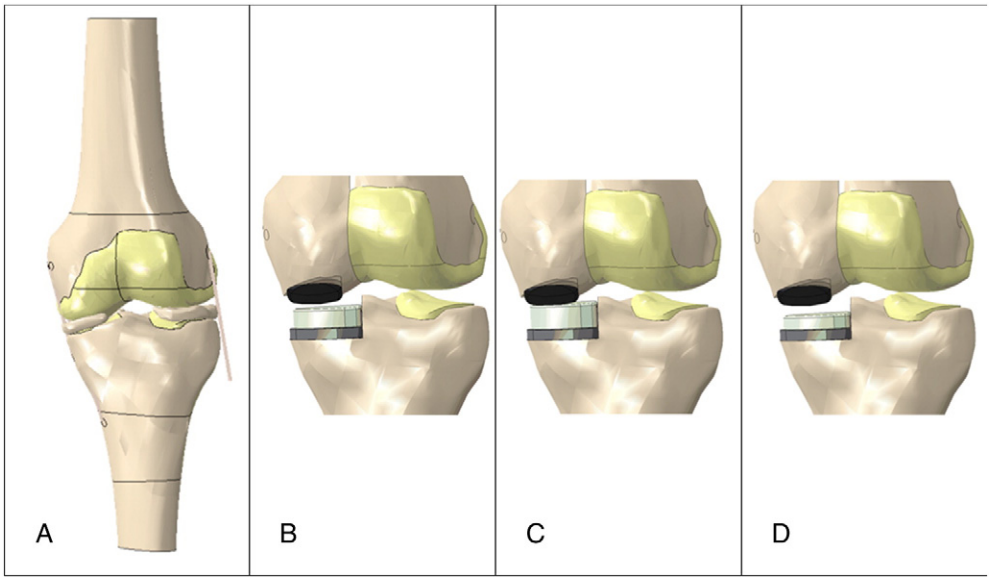

Fig. 1. Knee configurations analyzed: (A) healthy configuration, (B) Balanced configuration (insert thickness 10 mm), (C) Overstuffing configuration (insert thickness 12 mm), (D) Understuffing configuration (insert thickness 8 mm).

A material-test machine, 858 Mini Bionix R II Test System, was used to apply the 2000 N compressive load to the same native knee joint used to define the FE geometries. The load was applied at a loading rate of 400 N/s in the experiments. Furthermore, the constraints of the femur and tibia were equal to those in the FE models.

The native knee joint was loaded and the load distribution between medial and lateral compartment of the knee joint was measured simultaneously using Tekscan I-ScanTM model 6900 pressure measurement system (I-ScanTM, Tekscan, Inc., South Boston, MA) [52]. The experimental setup is shown on Fig. 2. To evaluate the reproducibility of the data, consisting of simultaneous measurements in both compartments of the knee joint, each specific experimental setup was recorded five times. After the experiments with the native knee joint, the experimental implantation of the UKA prosthesis was performed by an experienced orthopaedic surgeon. The sizes of both the tibial tray and the femoral component, implanted in the cadaveric knee, were the same to the one adopted in the FE models.

Fig. 2. Experimental setup.

Subsequently, the balanced knee joint was acquired by implanting an insert of 10 mm, and the identical measurement protocol was followed. Next, two configurations of understuffing were examined by implanting an 8 mm and a 9 mm tibial insert. Afterwards, overstuffing was investigated by incorporation an 11 mm and a 12 mm tibial insert. This specific sequence of experimental tests was determined in order to avoid tests wherein the ligaments were stretched excessively by previous tests.

Results

The relative load distribution between the medial and lateral compartments of the knee joint was measured in the numerical models as well as in the experimental tests. The average percentages of the load, carried by the lateral compartment, in all the different experimental configurations are shown in blue in Fig. 3. Good agreement is shown among the experimental results and the ones of the model with the ligaments. In the experimental tests, the standard deviation for each specific configuration never exceeded 3.9%. The transferred load (in N) in each compartment of the knee joint is reported in Table 3.

The strains in the aMCL, pMCL and LCL for all the different configurations are reported in Fig. 4. The strains in the collateral ligaments changed considerably especially in the balanced (120%) and overstuffed configurations (230%) (Fig. 4). The knee varus/valgus alignment was also measured in this study as the rotational angle of the femur in the coronal plane. The Valgus deformity angle plot for all the configurations, reported in Fig. 5, shows that every configuration after UKA, due to the increase of the stiffness in the medial side introduced by the present of the device, ended with a valgus alignment configuration. Valgus alignment was more pronounced when the thickness of the insert increased.

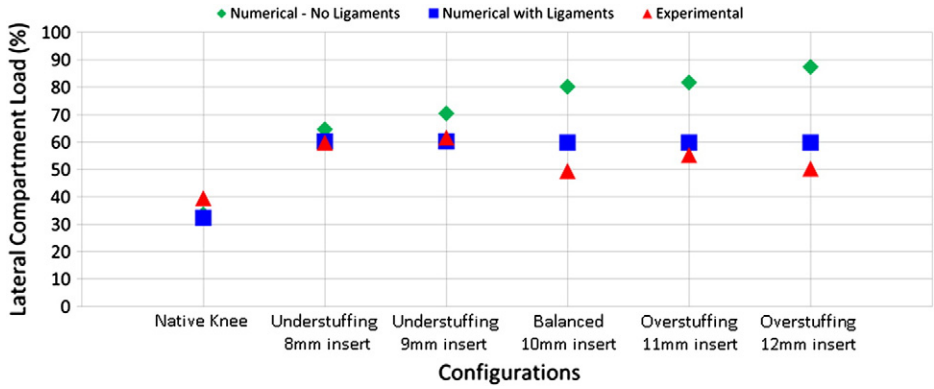

Fig. 3. Lateral compartmental load percentage for all the configurations under investigation, for the analyzed numerical models, with and without ligaments, and for the experimental tests.

Fig. 6 illustrates the Von Mises stresses distribution in the tibial region of the healthy knee model and how it changes after the implantation of a UKA. As shown, the stress values in the cancellous bone in the lateral condyle of the tibia increased after UKA up to 140%. Moreover, the stresses in the cortical bone of the tibia in the medial condyle increased as well (115%). On the other hand, the stresses in the cancellous bone beneath the tibial tray considerably decreased.

Finally, a graphical validation was performed by fitting two photos of a specific experiment to the final shape calculated in the corresponding FE model. This was done by taking photos of the unloaded and loaded configuration of the native knee following UKA including a 12 mm insert. Fig. 7 illustrates the photos with the outlined FE models of the unloaded as well as the loaded state.

Discussion

The load distribution between the lateral and medial compartments of the knee in the experiments with the native knee approximated the distribution found in literature. Investigating the contact force distribution in the knee joint, several research papers reported values of 800 N and 1200 N, in the lateral and medial compartment respectively; consequently, the distribution of the total force, in these models, between the two compartments is 40% on the lateral and 60% on the medial compartment [28,50,53]. We have good agreement with these results as the average percentage of the load that was transferred on the lateral side in the native knee in this study was 39.5%.

Looking at the load distribution in the experimental test, good agreement was found among the experimental results and the numerical one once the ligaments are included in the study, while the numerical knee model without ligaments overestimated the load on the lateral side (Fig. 3).

Even though the percentage of the load in the lateral compartment remained almost constant in the five configurations with the ligaments included, the absolute values of the load in the lateral compartment increased up to 125%. The load in the medial compartment raised as well in the knee models including the ligaments.

The deviation of FE models lacking the collateral ligaments was more expressed when the size of the insert in the FE model increased. This is clearly reported in Fig. 3. The transferred load in the medial compartment of the knee models lacking collateral ligaments decreased due to the increase in valgus deformity (Fig. 5) as well as the absence of the MCLs to counteract this deformity. Hence the inclusion of the collateral ligaments in the numerical models is fundamental in obtaining a physiological load distribution.

As already reported, every configuration after UKA ended with a valgus deformity (Fig. 5), even if the balanced native knee model has a correct alignment (valgus rotation 0°). This phenomenon could be explained by the difference in stiffness between the medial and lateral compartments of the knee following UKA. On the lateral side, the cartilage layer of both tibia and femur has an elastic modulus of 15 MPa. In contrast to the cartilage layers, the tibial articular insert has an elastic modulus of 685 MPa. Consequently, the Young's Modulus of medial and lateral compartments differs by more than one order of magnitude. So the materials in each compartment deform according to their elastic modulus. This problem is not present in a TKA because the total articular surface of the knee joint is restored and the stiffness in both compartments is equal. As a consequence of the stiffness difference, the valgus deformity induced a decreased strain in the LCL and an increased strain in the MCLs (Fig. 4).

The initial strains of the collateral ligaments in the healthy knee models were taken from literature, and they corresponded to the physiological strains at full extension [32,33,35,40]. As soon as the ligaments of the knee are stretched, they contribute to the total force acting between the femur and tibia. Hence, the total force acting in the knee joint of the FE models with ligaments exceeds the applied force of 2000 N.

The effects of the collateral ligaments on the load distribution in the knee models, including a UKA prosthesis, were represented in Fig. 3. The balanced configuration, in both the experiments and the FE model, with the tibial insert of 10 mm, had the aim to end with a balanced knee joint. Due to the difference in stiffness between

Table 3
Transferred Load (in N) in Each Compartment of the Knee Joint for the Numerical Simulation.

Configuration	Medial Side No Ligaments	Lateral Side No Ligaments	Medial Side With Ligaments	Lateral Side With Ligaments
Native Knee	1373	693	1608	746
Understuffing 8 mm insert	732	1328	933	1402
Understuffing 9 mm insert	610	1449	967	1462
Balanced 10 mm insert	476	1498	1012	1508
Overstuffing 11 mm insert	378	1678	1052	1563
Overstuffing 12 mm insert	263	1791	1086	1616

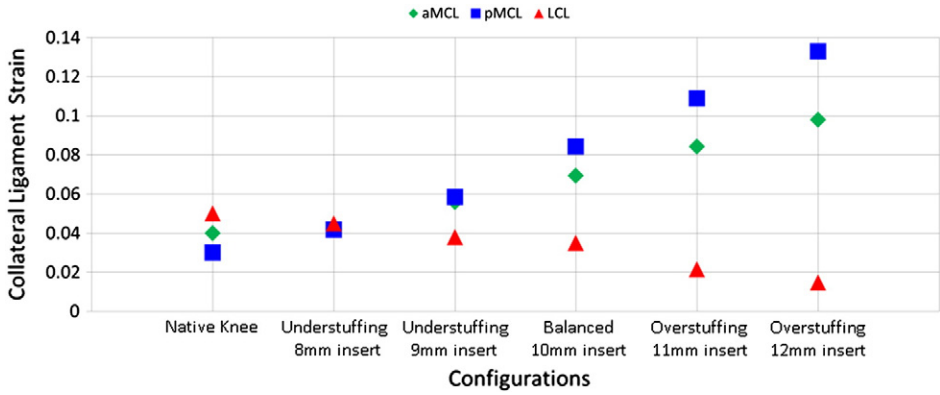

Fig. 4. Strain in the collateral ligaments of the knee model for all the investigated configurations during the application of the load.

cartilage–cartilage interaction and metal–UHMWPE interaction, the loaded knee was no longer balanced even though the knee joint was balanced in unloaded state. The deformity induced by loading had two consequences, as confirmed by the outcomes of the numerical models: firstly, the percentage of load that was transferred in the lateral compartment increased; secondly, the strain in the aMCL and pMCL raised and the strain in the LCL decreased. Hence, when a surgeon balances a knee during UKA in an unloaded state, the knee will no longer be balanced once it is loaded.

Godest et al (2002) described the role of the surrounding tension within the soft tissues and they reported that both the relative position of the components and the tension of the surrounding soft tissues have an impact on the results [44]. Moreover, Raminaraka et al (2005) agreed also that the stresses inside the soft structures as well as joint bearing forces are required to better understand the biomechanical behaviour of the knee [40]. This study confirmed the conclusions of the two previous studies.

This study demonstrated not only that the polyethylene thickness plays an important role in the knee following UKA, but also that previous studies, including a UKA prosthesis in the FE models, have to be critically evaluated. For instance Sawatari et al (2005) performed a three-dimensional FEA of UKA [54]. In particular they investigated the influence of the tibial tray orientation in the coronal plane. They concluded that it was beneficial to place the tibial component with a slight valgus inclination. However, they did not analyze the stresses in the lateral compartment of the knee and the ligaments were omitted additionally in their models.

In case of overstuffing, the unloaded knee was already unbalanced due to an oversized tibial insert. This was simulated by the implantation of a tibial insert of size 11 mm or 12 mm. The effects of overstuffing were clearly noticeable in the results.

The valgus deformity due to overstuffing was intensified by the difference in stiffness of the materials in both compartments. Although the percentage of load that was transferred through the lateral compartment in the FE models remained almost equal to the outcome of the balanced configuration, the absolute values of the transferred load in the lateral compartment increased (Table 3). On the other hand, the load on the medial side of the joint rises as well (Table 3). This was mainly caused by the MCLs, in which the strains raised sharply. The MCLs extended in contrast to the LCL, whose length further declined. This was clearly visible in Fig. 4. Additionally, a graphical validation was performed in case of overstuffing with 12 mm insert (Fig. 7) that also confirm the final valgus deformity of the knee.

Understuffing was obtained by inserting an undersized tibial insert. It was simulated by the placement of an insert of 9 mm or 8 mm. Understuffing in UKA is a well-known situation in orthopaedic surgery; yet, the biomechanical behavior of understuffing had never been investigated in detail. It has been postulated that a medial overcorrection leads to an accelerating degeneration in the lateral compartment and it has been reported that an overall undercorrection would prevent this [16,55]. It is generally accepted that for a medial unicompartmental arthroplasty, the knee should be slightly undercorrected. This concept is supported to some extent by the results of this study, because the valgus deformity was less pronounced in the understuffed configurations. However, the load distribution and the strains in the ligaments did not match the conditions of the healthy knee, hence, an implantation of a UNI always alter the biomechanics of the knee joint.

Loosening of the prosthetic components is one of the main three problems in UKA postoperatively. It is caused by excessive stresses in both cortical and cancellous bone, which lead to stress shielding. The

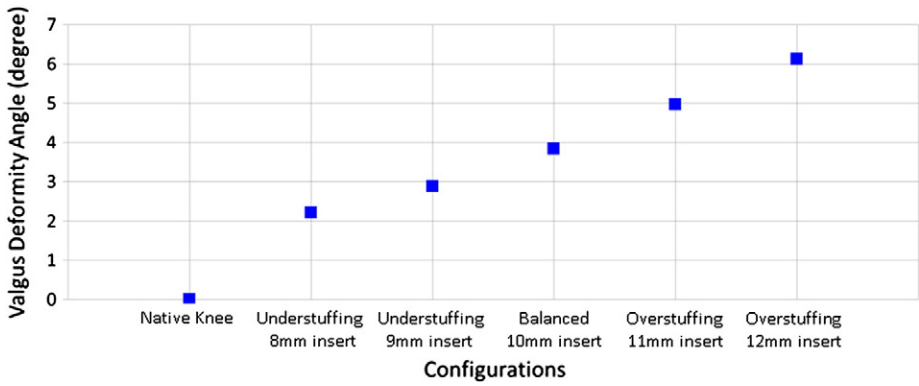

Fig. 5. Valgus Deformity Angle of the knee model for all the investigated configurations during the application of the load.

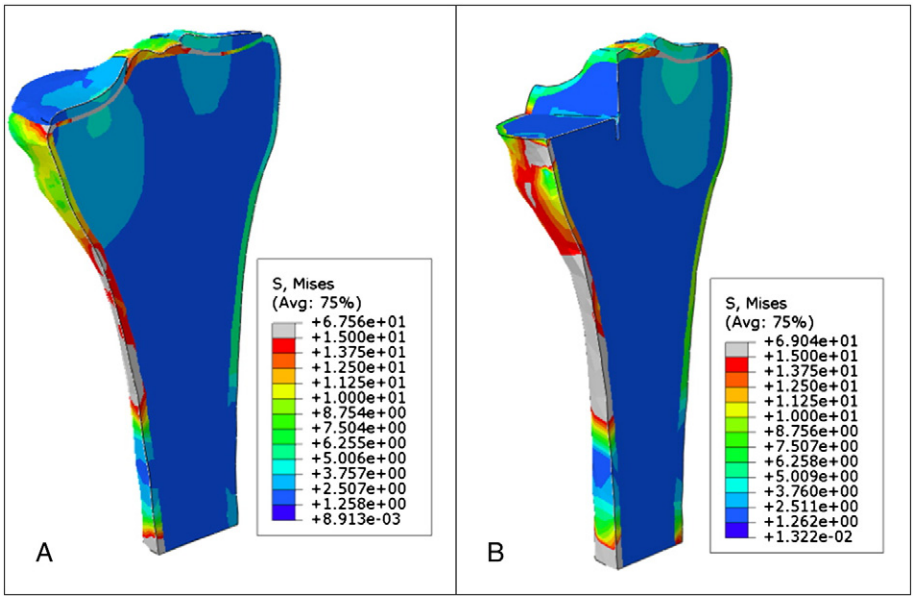

Fig. 6. Von Mises Stress distribution in the tibia: (A) healthy configuration, (B) Balanced configuration (insert thickness 10 mm).

main cause of the latter is the large difference in Young's modulus between the tibial tray material and the surrounding bone. In contrast to TKA, the interface between tibial tray and tibial bone is significantly smaller. This implies that the underlying bone stresses are considered to be more sensitive to component misalignment and malpositioning. In our FE models of UKA, the stresses in the cancellous bone underneath the tibial tray declined sharply compared with the stresses in the healthy knee model, as represented in Fig. 6. This was due to the high stiffness of the tibial tray which redistributed the load between cancellous and cortical bone. The tibial tray redirected practically the entire load on the medial side to the cortical bone just because the elastic modulus of the cortical bone is much larger than the elastic modulus of the cancellous bone. The balanced configuration as well as overstuffing and understuffing induced an altered stress distribution in the tibial bone.

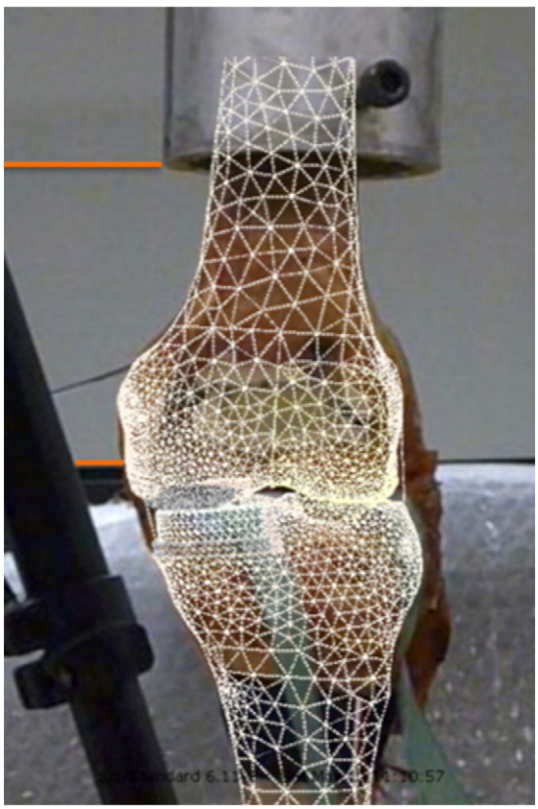

Fig. 7. Graphical validation, pictures of an experiment with the knee following UKA (insert 12 mm), together with the outline of the corresponding FE model during a loaded test.

The increased bone stresses in the cortical bone and the decreased bone stresses in the cancellous bone around the tibial tray could lead to loosening of the tibial tray and could induce pain. Furthermore, the developed FE models of this study provided more insight into the biomechanical processes inside the knee structures after UKA and the models released information which could not be obtained by experiments.

Several assumptions were made in the FE models; firstly, the geometries of the different structures of the developed FE models are patient specific and originated from CT and MRI images. The segmentation of the structures in the CT and MRI sequences was semi-automatic. The dimensions of bony structures approached very well the physiological dimensions; however the geometries of the soft structures were more difficult to determine due to the low resolution of the MRI sequence. The cartilage layers were determined on the basis of CT and MRI images. In contrast to the cartilage layers, the geometry of the menisci was less precisely defined. Moreover, the ligaments were modelled as beams. Secondly, the material models of the different structures in this study incorporated several assumptions, although the behavior of the structures approximated their natural behavior. The material properties of the bony structures as well as the soft tissues were assumed linear elastic and homogeneous. As it is well known, the cortical as well as the cancellous bones contain spatial inhomogeneities in their properties [28]. Some studies in the past already incorporated a Neo-Hookean material model to predict the non-linear stress–strain behavior of the ligaments that undergo large deformations [33,56]. Finally, the degrees of freedom of the different parts in the experiments were limited. Only the available degrees of freedom were consequently incorporated in the FE models. Because the knee was placed in full extension and internal/external rotation was constrained in the experiments, the cruciate ligaments were omitted in the FE models. With respect to the experiments, two main limitations need to be highlighted. First, the experimental analysis was performed on a fresh-frozen cadaver and not on a real

leg. However, a recent study [57] demonstrated that repeatedly freezing and thawing tendons between −80° C and room temperature do not significantly influence their biomechanical properties. Therefore we believe that the biomechanical behavior of the knee tissues in a fresh frozen cadaver specimen is quite comparable to that in a live patient. Secondly, the study refers to a static condition (full extension) and not to a dynamic condition. The latter is currently under investigation. However, our results are in agreement with another recent dynamic study [58] in which subtle but significant kinematic differences were found between six healthy knees and the same knees after UKA. Also in this study, the knees showed an increase in valgus tilt after UKA. Moreover, the authors conclude that one of reasons of the kinematic changes was probably due to the mismatch in stiffness introduced by UKA.

Conclusions

In this study a numerical model of an intact cadaveric knee specimen, was developed and validated with experimental test. It was used to quantify the tibial stresses and ligament strains induced by a medial UKA. We found alterations in the tibial stress distribution and the collateral ligament strains and could explain this by the change in stiffness between the medial and the lateral compartment in the knee induced by the UKA; this was found both numerically and experimentally. A considerable increase in medial collateral ligament strain was observed especially in the balanced and overstuffed configurations. This study may help explain the pain and progression of disease that can occur following unicompartmental knee arthroplasties.

Reference

1. Brooks PM. Impact of osteoarthritis on individuals and society: how much disability? Social consequences and health economic implications. Curr Opin Rheumatol 2002;14:573.
2. Reginster JY. The prevalence and burden of arthritis. Rheumatology 2002;41:3.
3. Suggs JF, Li G, Se Park, et al. Knee biomechanics after UKA and its relation to the ACL — a robotic investigation. J Orthop Res 2006;24:588.
4. Berger RA, Nedeff DD, Barden RM, et al. Unicompartmental knee arthroplasty. Clinical experience at 6- to 10-year followup. Clin Orthop Relat Res 1999;367:50.
5. Cartier P, Sanouiller JL, Grelsamer RP. Unicompartmental knee arthroplasty surgery. 10-year minimum follow-up period. J Arthroplasty 1996;11:782.
6. Murray DW, Goodfellow JW, O'Connor JJ. The Oxford medial unicompartmental arthroplasty: a ten-year survival study. J Bone Joint Surg Br 1998;80:983.
7. Berger RA, Meneghini RM, Jacobs JJ, et al. Results of unicompartmental knee arthroplasty at a minimum of ten years of follow-up. J Bone Joint Surg Am 2005;87:999.
8. Squire MW, Callaghan JJ, Goetz DD, et al. Unicompartmental knee replacement a minimum 15 year follow up study. Clin Orthop Relat Res 1999;367:61.
9. Riebel GD, Werner FW, Ayers DC, et al. Early failure of the femoral component in unicompartmental knee arthroplasty. J Arthrop 1995;10:615.
10. Aleto TJ, Berend ME, Ritter MA, et al. Early failure of unicompartmental knee arthroplasty leading to revision. J Arthrop 2008;23:159.
11. Parratte S, Pauly V, Aubaniac JM, et al. No long-term difference between fixed and mobile medial unicompartmental arthroplasty. Clin Orthop Relat Res 2012;470:61.
12. Price AJ, Short A, Kellett C, et al. Ten-year in vivo wear measurement of a fully congruent mobile bearing unicompartmental knee arthroplasty. J Bone Joint Surg Br 2005;87:1493.
13. Epinette JA, Brunschweiler B, Mertl P, et al. Unicompartmental knee arthroplasty modes of failure: wear is not the main reason for failure: a multicentre study of 418 failed knees. Orthop Traumatol Surg Res 2012;98:124.
14. Lygre SH, Espehaug B, Havelin LI, et al. Pain and function in patients after primary unicompartmental and total knee arthroplasty. J Bone Joint Surg Am 2010;92:2890.
15. Jeer PJ, Keene GC, Gill P. Unicompartmental knee arthroplasty: an intermediate report of survivorship after the introduction of a new system with analysis of failures. Knee 2004;11:369.
16. Chang TW, Yang CT, Liu YL, et al. Biomechanical evaluation of proximal tibial behavior following unicondylar knee arthroplasty: modified resected surface with corresponding surgical technique. Med Eng & Phys 2011;33:1175.
17. Yang KY, Yeo SJ, Lo NN. Stress fracture of the medial tibial plateau after minimally invasive unicompartmental knee arthroplasty: a report of 2 cases. J Arthrop 2003;18:801.
18. Buechel FF, Keblish PA, Lee JM, et al. Low contact stress meniscal bearing unicompartmental knee replacement: long term evaluation of cemented and cementless results. J Orthop Rheumatol 1994;7:31.
19. Simpson DJ, Price AJ, Gulati A, et al. Elevated proximal tibial strains following unicompartmental knee replacement—a possible cause of pain. Med Eng & Phys 2009;31:752.
20. Hamilton WG, Ammeen D, Engh Jr CA, et al. Learning curve with minimally invasive unicompartmental knee arthroplasty. J Arthrop 2010;25:735.
21. Perkins TR, Gunckle W. Unicompartmental knee arthroplasty. 3- to 10- year results in a community hospital setting. J Arthrop 2002;17:293.
22. Marmor L. Unicompartment knee arthroplasty: ten to 13 year follow-up study. Clin Orthop Relat Res 1988;226:14.
23. Kozinn S, Scott R. Unicondylar knee arthroplasty: current concepts review. J Bone Joint Surg Am 1989;71:145.
24. Kennedy W, White R. Unicompartment arthroplasty of the knee: post-operative alignment and its influence on overall results. Clin Orthop Relat Res 1991;271:96.
25. Laskin RS. Unicompartmental tibiofemoral resurfacing arthroplasty. J Bone Joint Surg Am 1978;60:182.
26. Innocenti B, Pianigiani S, Labey L, et al. Contact forces in several TKA designs during squatting: a numerical sensitivity analysis. J Biomech 2011;44:1573.
27. Pianigiani S, Chevalier Y, Labey L, et al. Tibio-femoral kinematics in different total knee arthroplasty designs during a loaded squat: a numerical sensitivity study. J Biomech 2012;45:2315.
28. Sarathi Kopparti P, Lewis G. Influence of three variables on the stresses in a three-dimensional model of a proximal tibia-total knee implant construct. Biomed Mater Eng 2007;17:19.
29. Rho YJ, Kuhn-Spearing L, Zioupos P. Mechanical properties and the hierarchical structure of bone. Med Eng & Phys 1998;20:92.
30. Kayabasi O, Ekici B. The effects of static, dynamic and fatigue behavior on threedimensional shape optimization of hip prosthesis by finite element method. Mater Des 2006;28:2269.
31. Hopkins AR, New AM, Rodriguez-y-Baena F, et al. Finite element analysis of unicompartmental knee arthroplasty. Med Eng & Phys 2010;32:14.
32. Peña E, Calvo B, Martinez MA, et al. A three-dimensional finite element analysis of the combined behavior of ligaments and menisci in the healthy human knee joint. J Biomech 2006;39:1686.
33. Donahue TLH, Hull ML, Rashid MM, et al. How the stiffness of meniscal attachments and meniscal material properties affect tibio-femoral contact pressure computed using a validated finite element model of the human knee joint. J Biomech 2003;36:19.
34. Penrose JM, Holt GM, Beaugonin M, et al. Development of an accurate three-dimensional finite element knee model. Comput Methods Biomech Biomed Engin 2002;5:291.
35. Bendjaballah MZ, Shirazi-Adl A, Zukor DJ. Biomechanics of the human knee joint in compression: reconstruction, mesh generation and finite element analysis. Knee 1995;2:69.
36. LeRoux MA, Setton LA. Experimental and biphasic fem determinations of the material properties and hydraulic permeability of the meniscus in tension. J Biomechanic Eng 2002;124:315.
37. Blankevoort L, Huiskes R. Ligament–bone interaction in a three-dimensional model of the knee. J Biomech Eng 1991;113:263.
38. Pandy MG, Sasaki K, Kim S. A three-dimensional musculoskeletal model of the human knee joint. part 1: theoretical construct. Comput Methods Biomech Biomed Engin 1998;1:87.
39. Springer BD, Scott RD, Thornhill TS. Conversion of failed unicompartmental knee arthroplasty to TKA. Clin Orthop Relat Res 2006;446:214.
40. Ramaniraka NA, Terrier A, Theumann N, et al. Effects of the posterior cruciate ligament reconstruction on the biomechanics of the knee joint: a finite element analysis. Clin Biomech 2005;20:434.
41. Whittaker JP, Naudie DDR, McAuley JP, et al. Does bearing design influence midterm survivorship of unicompartmental arthroplasty? Clin Orthop Relat Res 2010;468:73.
42. Gleeson RE, Evans R, Ackroyd CE, et al. Fixed or mobile bearing unicompartmental knee replacement? A comparative cohort study. Knee 2004;11:379.
43. Unsworth A, Downson D, Wright V. The frictional behaviour of human synovial joints. I. Natural joints. J Lubrication Tech 1975;97:369.
44. Godest AC, Beaugonin M, Haug E, et al. Simulation of a knee joint replacement during a gait cycle using explicit finite element analysis. J Biomech 2002;35:267.
45. Soenen M, Baracchi M, De Corte R, et al. Stemmed TKA in a femur with a total hip arthroplasty: is there a safe distance between the stem tips? J Arthrop 2013; 28:1437.
46. Catani F, Innocenti B, Belvedere C, et al. The Mark Coventry Award: articular contact estimation in TKA using in vivo kinematics and finite element analysis. Clin Orthop Relat Res 2010;468:19.
47. van Jonbergen HP, Innocenti B, Gervasi GL, et al. Differences in the stress distribution in the distal femur between patellofemoral joint replacement and total knee replacement: a finite element study. J Orthop Surg Res 2012;7:28.
48. Innocenti B, Truyens E, Labey L, et al. Can medio-lateral baseplate position and load sharing induce asymptomatic local bone resorption of the proximal tibia? A finite element study. J Orthop Surg Res 2009;4:26.
49. Au AG, Raso VJ, Liggins AB, et al. A threedimensional finite element stress analysis for tunnel placement and buttons in anterior cruciate ligament reconstructions. J Biomech 2005;38:827.
50. Morrison JB. The mechanics of the knee joint in relation to normal walking. J Biomech 1970;3:51.
51. Walker PS, Blunn GW, Broome DR, et al. A knee simulating machine for performance evaluation of total knee replacements. J Biomech 1997;30:83.
52. Wirz D, Becker R, Li SF, et al. Validation of the tekscan system for statistic and dynamic pressure measurements of the human femorotibial joint. Biomedizinische Technik Biomed Engin 2002;47:195.

53. Beaupre GS, Vasu R, Carter DR, et al. Epiphyseal-based designs for tibial plateau components—ii. stress analysis in the sagittal plane. J Biomech 1986;19:663.
54. Sawatari T, Tsumura H, Iesaka K, et al. Threedimensional finite element analysis of unicompartmental knee arthroplasty—the influence of tibial component inclination. J Orthop Res 2005;23:549.
55. Borus T, Thornhill T. Unicompartmental knee arthroplasty. J Am Acad Orthop Surg 2008;16:9.
56. Gardiner JC, Weiss JA. Subject-specific finite element analysis of the human medial collateral ligament during valgus knee loading. J Orthop Res 2003; 21:1098.
57. Arnout N, Myncke J, Vanlauwe J, et al. Acta Otrhop Belg 2013;79:435.
58. Heyse TJ, El-Zayat BF, De Corte R, Chevalier Y, Scheys L, Innocenti B, Fuchs-Winkelmann S, Labey L. UKA closely preserves natural knee kinematics in vitro. KSSTA Journal (in press).